Catalysis Today 138 (2008) 228–234

Contents lists available at ScienceDirect

Catalysis Today

journal homepage: www.elsevier.com/locate/cattod

The water-gas shift reaction on Pt/γ-Al_2O_3 catalyst: *Operando* SSITKA-DRIFTS-mass spectroscopy studies

Christos M. Kalamaras, George G. Olympiou, Angelos M. Efstathiou *

Department of Chemistry, Heterogeneous Catalysis Laboratory, University of Cyprus, P.O. Box 20537, Nicosia CY 1678, Cyprus

ARTICLE INFO

Article history:
Available online 21 July 2008

Keywords:
Water-gas shift reaction
Supported-Pt catalyst
SSITKA
DRIFTS
Catalytic reaction mechanisms
Operando catalytic studies

ABSTRACT

Steady-state isotopic transient kinetic analysis (SSITKA) experiments coupled with *in situ* DRIFTS and mass spectrometry (*operando*) were performed *for the first time* to study essential mechanistic aspects of the water-gas shift reaction (WGSR) over a 0.5 wt.% Pt/γ-Al_2O_3 catalyst. The chemical structure of *active* and *inactive reaction intermediate species* present in the carbon-path (“C-path”) from CO to the CO_2 product gas (use of ^{13}CO) and in the hydrogen-path (“H-path”) from H_2O to the H_2 product gas (use of D_2O) of the reaction mechanism were determined. In addition, the concentrations (μmol/g) of *active* species in both the “C-path” and “H-path” of the WGSR at 350 °C were measured. Based on the large concentration of active species present in the “H-path” (OH/H located on the alumina support), the latter being larger than 28 equivalent monolayers of the exposed Pt metal surface, the small concentration of OH groups along the periphery of metal-support interface, and the significantly smaller concentration (μmol/g) of active species present in the “C-path” (adsorbed CO on Pt and COOH species on the alumina support and/or the metal-support interface), it might be suggested that diffusion of OH/H species on the alumina support surface towards Pt catalytic sites present in the “H-path” of reaction (back-spillover process) might be considered as a slow reaction step. The latter process was evidenced after conducting the WGS reaction (CO/H_2O) in a partially deuterated alumina surface (Pt/γ-Al_2O_3). At least *two kinds* of formate (–COOH) species residing on the alumina surface have been identified, one of which was *active* and leads to the formation of CO_2(g) and H_2(g), whereas the other kind(s) is/are considered as *inactive* (spectator) adsorbed reaction intermediate species.

1. Introduction

Low- and high-temperature operating water-gas shift reaction, WGSR ($CO + H_2O \leftrightarrows CO_2 + H_2$) catalysts, e.g., Fe_3O_4/Cr_2O_3 and $Cu/ZnO/Al_2O_3$, respectively, are used for industrial hydrogen production [1–3]. These catalysts, however, are pyrophoric and deactivate if exposed to air and condensed water. Attempts are now focused towards the development of low-loading robust noble metal-based catalysts that are non-pyrophoric with high activity at low-temperatures and which will result in a CO content less than 5 ppm in the hydrogen gas stream produced when the latter is going to be used in hydrogen fuel cells [1,4]. This goal will be greatly facilitated if one understands, to a good extent, the important aspect of the mechanism of the WGSR over supported noble metal catalysts.

A number of different mechanisms for the WGSR over supported catalysts on metal oxides have been proposed and disagreements exist about the important active intermediate species involved and the rate-determining step [5,6]. Two reaction mechanisms were mainly proposed [4,7–17]: (i) the *regenerative* mechanism (redox), and (ii) the *adsorptive* mechanism (non-redox). In the regenerative mechanism [7–12] CO adsorbs on the noble metal which then diffuses on the support and reacts with lattice oxygen to form CO_2(g). Water adsorbs and dissociates mainly on the reduced support sites, thus re-oxidizing the support sites and producing H_2(g). In the adsorptive mechanism [13–17], CO and H_2O were proposed to adsorb on catalyst active sites to form surface carbon-containing intermediates (e.g., formates, carbonates and bicarbonates), which finally decompose to form H_2 and CO_2. The nature and true location of these active intermediates (support, metal-support interface or metal) are still controversial. For example, formate and carbonate species were proposed to be important WGSR intermediates over various supported noble metals [4,10,15–18]. Grenoble et al. [18] proposed formates as being active intermediate over alumina-supported group VIIB, VII and IB metals, while Ricote et al. [19] proposed that one of the metal’s main roles is to favour the formation of reactive surface hydroxyl groups on the oxide support which can lead to an increased rate of formation of formate species. Meunier et al. [20]

---

* Corresponding author. Tel.: +357 22 892776; fax: +357 22 892801.
E-mail address: efstath@ucy.ac.cy (A.M. Efstathiou).

0920-5861/$ – see front matter © 2008 Elsevier B.V. All rights reserved.
doi:10.1016/j.cattod.2008.06.010

have recently proposed that formates can potentially be WGSR intermediates over Pt/CeO_2 above 200 °C, whereas formates were merely reaction spectator species below this temperature.

In the present work, for *the first time* Steady-State Isotopic Transient Kinetic Analysis (SSITKA) experiments coupled with DRIFTS and mass spectrometry (*operando*) have been performed to probe the *chemical structure* of *active* and *inactive* (spectator) reaction intermediates found in the carbon-path (C-path) of the WGSR over a 0.5 wt.% $Pt/\gamma\text{-}Al_2O_3$ catalyst and to provide mechanistic information on the role of formate species in this reaction pathway. The *surface concentrations* (μmol/g, θ (based on surface Pt)) of *active* "H-containing" and "C-containing" surface reaction intermediates were also measured by *in situ* SSITKA-Mass spectrometry experiments. The *back-spillover* of OH/H species from the alumina support to the Pt surface was probed by transient D-isotopic experiments. This important information allowed for proper discussion of crucial mechanistic issues of the reaction at hand.

2. Experimental

2.1. Catalyst preparation and characterization

The alumina-supported Pt catalyst (0.5 wt.%) was prepared by impregnating γ-alumina (5.8 nm mean pore diameter, 148 $m^2\,g^{-1}$, 150 mesh particle size) with an aqueous solution of $Pt(NH_3)_2(NO_2)_2$ (Aldrich) [21]. The Pt dispersion (%D) in the catalyst was determined by selective H_2 chemisorption at 25 °C followed by TPD in He flow (30 NmL/min) and a heating rate, β = 30 °C/min, where it was found to be 48% or 12.3 μmol Pt_s/g [21]. Prior to this experiment the fresh catalyst sample (0.3 g) was calcined in a $20\%O_2/He$ (50 NmL/min) gas mixture at 500 °C for 2 h and then reduced in pure H_2 (30 NmL/min) at 300 °C for 2 h.

2.2. SSITKA-mass spectrometry studies

The isotopes used in the SSITKA experiments were ^{13}CO (99.5 at% ^{13}C, Spectra Gases) and deuterium oxide (D_2O) (99.96 at% D, Aldrich). SSITKA experiments were performed using two HPLC pumps (GILSON 307) for the addition of H_2O and D_2O to the reactor feed stream in the apparatus described elsewhere [22]. SSITKA experiments performed in order to follow the "H-path" of reaction involved the switch $3\%CO/10\%H_2O/Ar/Kr$ (30 min, 350 °C) → $3\%CO/1\%D_2O/Ar$ (350 °C, t), while those to follow the "C-path" of reaction involved the switch $3\%^{12}CO/10\%H_2O/Ar/He$ (30 min, 350 °C) → $3\%^{13}CO/10\%H_2O/Ar$ (350 °C, t). More details on the SSITKA experiments and the micro-reactor used were reported [21,22]. The mass of the alumina-supported Pt was 0.1 g diluted with 0.4 g of silica, the total flow rate of the reaction feed stream was 200 NmL/min, and the total pressure was about 1 atm. Under these conditions the CO conversion was below 20%.

2.3. Operando SSITKA-DRIFTS-mass spectrometry studies

Operando studies were performed in a specially designed gas flow-system where the response time of the DRIFTS reactor cell (~40 mg Pt/Al_2O_3) estimated from the Ar transient response curve to the switch $10\%H_2O/He$ → $10\%H_2O/1\%Ar/He$ (100 mL/min) was about 5 s [23,24]. A PerkinElmer FTIR spectrometer (Spectrum GX) equipped with a high-temperature/high-pressure temperature controllable DRIFTS cell (Harrick, Praying Mantis) with ZnSe windows was used for the *in situ* recording of IR spectra. Signal averaging was set to 50 scans per spectrum and the spectra were collected at the rate of 1 scan/s at a 2 cm^{-1} resolution in the 4000–800 cm^{-1} range. The collected DRIFTS spectra were smoothed in order to remove high frequency noise if necessary, and further analyzed using the software Spectrum® (PerkinElmer) for Windows. Deconvolution of the thus derived DRIFTS spectra was performed according to reported guidelines [25]. The background spectrum of the solid catalyst was taken under $10\%H_2O/Ar$ flow (100 mL/min) at the desired reaction temperature. The IR data were reported as log 1/R (absorbance mode) using the relationship, $R = I/I_o$. Here, R is the catalyst sample reflectance, I_o is the absorbance intensity of the solid catalyst itself, and I is the absorbance intensity of both the solid catalyst and adsorbate under reaction conditions. The function log 1/R was found to give a better linear correlation of the band area against surface coverage than that given by the Kubelka-Munk function for strongly absorbing media [26].

The product gas from the exit of DRIFTS reactor cell was directed to the mass spectrometer (Balzer, Omnistar, 1–300 amu) for recording the *transient evolution* of gaseous H_2, CO and CO_2 (normal and isotope-containing ^{13}C species) (*operando* studies). SSITKA experiments with ^{13}CO (99.5 at% ^{13}C, Spectra Gases) performed using the DRIFTS reactor cell involved the switch $3\%^{12}CO/10\%H_2O/Ar/He$ (350 °C, 30 min) → $3\%^{13}CO/10\%H_2O/Ar$ (350 °C, t) at a total flow rate of 100 NmL/min in order to follow the "C-path" of the WGSR.

2.4. Transient isotopic experiments to probing –OH/H back-spillover

The back-spillover of labile hydroxyl groups (–OH) and H species from the alumina support to the Pt metal surface was

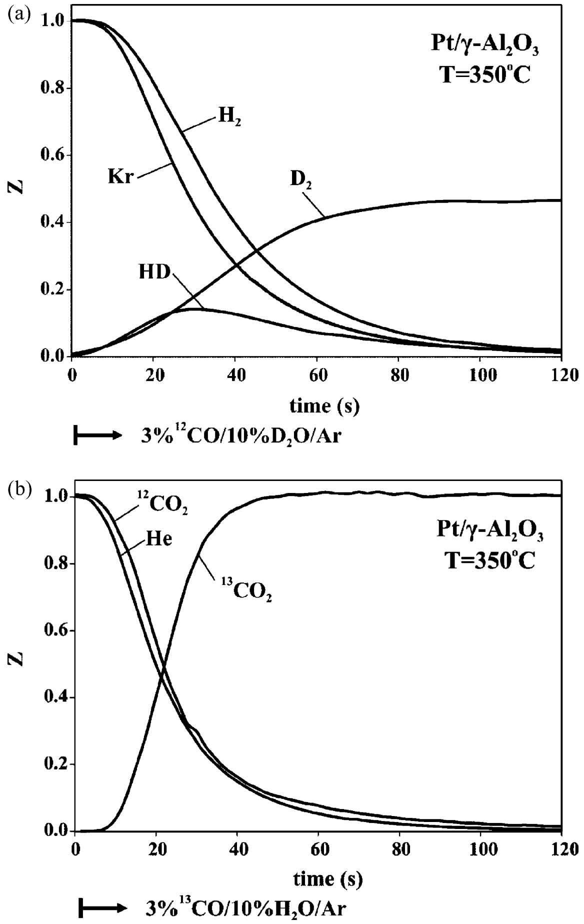

Fig. 1. SSITKA-mass spectrometry experiments performed to quantify the "H-path" (a) and the "C-path" (b) of the WGS reaction on 0.5 wt.% $Pt/\gamma\text{-}Al_2O_3$ catalyst at 350 °C. Gas delivery sequence: (a) $3\%CO/10\%H_2O/Ar/Kr$ (30 min) → $3\%CO/10\%D_2O/Ar$ (t); (b) $3\%^{12}CO/10\%H_2O/Ar/He$ (30 min) → $3\%^{13}CO/10\%H_2O/Ar$ (t).

probed according to the following experimental procedure: 10%D_2O/Ar (500 °C, 30 min) → Ar (500 °C, 10 min) → 3%CO/10%H_2O/Ar (500 °C, t). The effluent stream from the quartz micro-reactor was directed to a mass spectrometer (Omnistar, Balzer) for continuous monitoring of the mass numbers (m/z) 2, 3 and 4 for H_2, HD and D_2, respectively [21,22]. The amount of catalyst (0.1–0.2 mm particle size) used was 0.5 g, and the flow rate of CO/H_2O/Ar gas mixture was 200 NmL/min.

3. Results and discussion

3.1. SSITKA-mass spectrometry

Fig. 1a presents dimensionless transient gas concentration response curves, Z, of H_2, HD, D_2 and Kr obtained after the isotopic switch 3%CO/10%H_2O/Ar/Kr (350 °C, 30 min) → 3%CO/10%D_2O/Ar (350 °C, t) was made in a micro-reactor connected to the mass spectrometer. The dimensionless concentration Z corresponds to the fraction of the ultimate change as a function of reaction time, t. Thus, Z is defined by

$$Z(t) = \frac{y(t)}{y_{\mathrm{s.s}}} \tag{1}$$

where, $y(t)$ is the mole fraction of a given isotopic gaseous species (H_2, D_2 or HD) at time t under the isotopic gas mixture, and $y_{\mathrm{s.s}}$ is the mole fraction of H_2(g) under the non isotopic gas mixture at steady-state. The decay of Kr gas concentration shown in Fig. 1a was used to monitor the gas phase hold-up of the system [24]. Kr gas was used instead of He in order to avoid the overlap in the signal of $m/z = 4$ due to He^+ and D_2^+ ions in the mass spectrometer analysis. At a given time, t, the sum of Z_i's for the three di-hydrogen isotopic species should be equal to one if a D-isotopic kinetic effect were absent. However, as seen in Fig. 1a this was not the case since a normal D-isotopic kinetic effect is observed ($R_{H_2}/R_{D_2} \sim 2.0$).

Fig. 1b presents similar dimensionless transient gas concentration response curves (Z) of $^{12}CO_2$, $^{13}CO_2$ and He obtained after the isotopic switch 3%^{12}CO/10%H_2O/Ar/He (350 °C, 30 min) → 3%^{13}CO/10%H_2O/Ar (350 °C, t) was made over the same catalyst sample. No ^{13}C-isotopic kinetic effect was observed since the steady-state rates of $^{12}CO_2$ and $^{13}CO_2$ under the two reaction mixtures were equal ($Z = 1$ at $t = 0$ and 120 s, Fig. 1b).

The concentration of active "H-containing" intermediate species, termed "H-pool", which is found in the mechanistic "hydrogen-path" ("H-path") of the WGSR was estimated based on the transient response curves of H_2, HD and Kr (Fig. 1a) details of which were previously reported [21]. The size of the surface "H-pool" was found to be 335 μmol H/g or 27.2 equivalent monolayers of surface Pt ($\theta_H = 27.2$, $Pt_s = 12.3$ μmol/g)). The concentration of active "C-containing" intermediate species ("C-pool") found in the mechanistic "C-path" of the WGSR was estimated based on the $^{12}CO_2$ and He response curves (Fig. 1b) [21]. The size of the "C-pool" was found to be 1.1 μmol C/g or equivalently, $\theta_C = 0.085$. The accuracy of the "H-pool" and "C-pool" amounts is considered to be within 5–10%.

The chemical nature of active "H-containing" intermediate species is considered to be likely that of labile hydroxyl groups (–OH), H (attached on surface O of alumina support, and/or adsorbed on the Pd surface), and formate (–COOH) species [13–17,21]. The latter species was clearly identified by the SSITKA-DRIFTS experiments to be presented next. The fact that the size of the "H-pool" measured was very large ($\theta_H = 27.2$) strongly suggests that OH/H species residing on the alumina support must participate in the reaction mechanism to form CO_2 and H_2. We have recently reported [21] that the size of the "H-pool" measured here is less than 35% of the monolayer value of –OH/H present on the alumina surface. Thus, *not all* –OH/H species present on the alumina are energetically able to participate in the reaction path of the WGSR. We have also demonstrated that this concentration of –OH/H species cannot be justified as being all present along the periphery of the Pt-alumina interface [21]. We have already proposed that there must be a region in the vicinity of Pt nanoparticles within which –OH/H species participate in the "H-path" of WGSR [21].

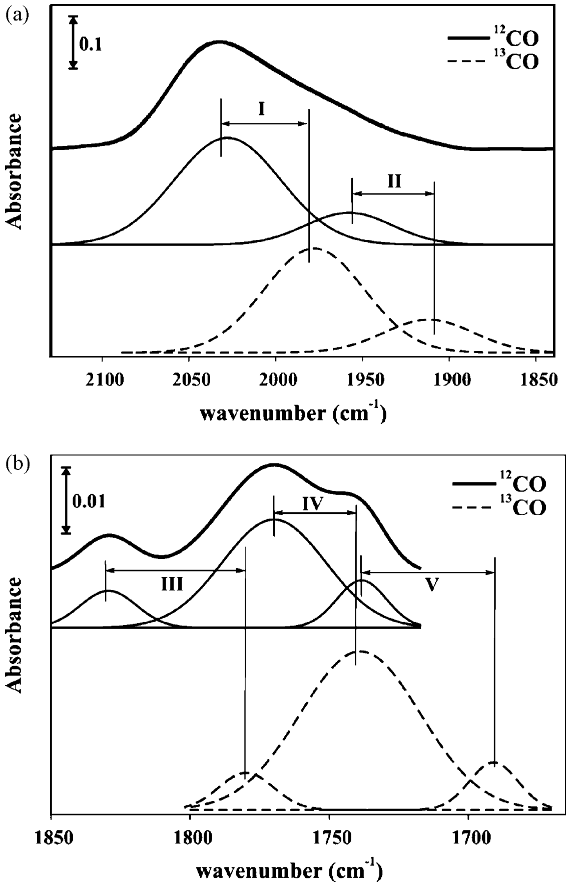

Fig. 2. DRIFTS spectra of linear adsorbed CO_L (a) and bridged adsorbed CO_B (b) recorded during *operando* SSITKA: 3%^{12}CO/10%H_2O/Ar/He (30 min) → 3%^{13}CO/10%H_2O/Ar (30 min) at 350 °C over the 0.5 wt.% Pt/γ-Al_2O_3 catalyst.

3.2. *Operando* SSITKA-DRIFTS-mass spectrometry

3.2.1. DRIFTS-WGS reaction

DRIFTS spectra in the 3050–1300 cm^{-1} range recorded on the 0.5 wt.% Pt/γ-Al_2O_3 catalyst during *operando* SSITKA-DRIFTS-mass spectrometer studies of the WGSR at 350 °C are presented in Figs. 2 and 3. The range of 2100–1850 cm^{-1} (Fig. 2a) corresponds to linear adsorbed CO [27–29], that of 1850–1670 cm^{-1} (Fig. 2b) to bridged CO species, that of 3050–2800 cm^{-1} (Fig. 3a) to formate (COOH) species (νCH and δCH + νOCO_a), whereas that of 1650–1300 cm^{-1} (Fig. 3c) to the O–C–O stretching vibrational mode of *formate*, *carbonate* and *carboxylate* species [16,17,30–32]. The various infrared bands observed in Fig. 2 and Fig. 3b under the ^{12}CO/H_2O and ^{13}CO/H_2O reaction mixtures after steady-state was achieved were obtained following deconvolution procedures [25].

The infrared bands centered at 2033 (type I) and 1957 (type II) cm^{-1}, respectively, correspond to *two kinds* of linear adsorbed carbon monoxide, CO_L [27–29]. Both IR bands were found to give the red isotopic shift (Fig. 2a, bottom graph). The infrared bands

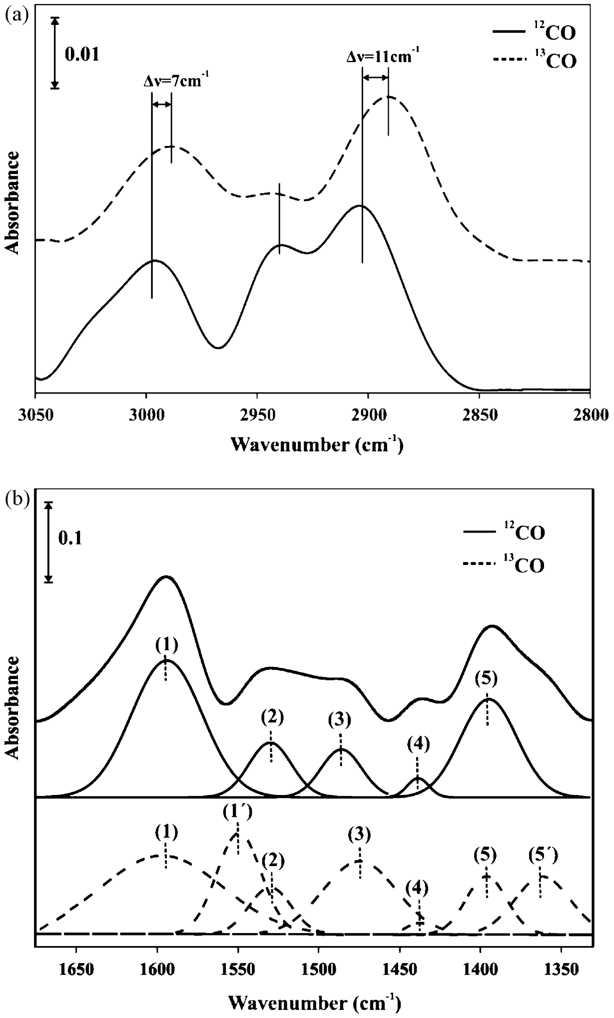

Fig. 3. DRIFTS spectra recorded in the 3050–2800 cm^{-1} range (a) and 1670–1320 cm^{-1} range (b) after steady-state WGS reaction conditions in 3%^{12}CO/10%H_2O/Ar/He and 3%^{13}CO/10%H_2O/Ar feed gas mixtures. Deconvolution and curve fitting of recorded IR spectra in (b) are also shown.

centered at 1829 (type III), 1771 (type IV) and 1740 cm^{-1} (type V), respectively, correspond to *three kinds* of adsorbed bridged carbon monoxide, CO_B species [27–29]. In this case also all three kinds of adsorbed CO_B observed gave the red isotopic shift (Fig. 2b, bottom graph).

Characteristic νCH stretching mode IR bands (2996, 2940, 2903 cm^{-1}) due to formate species on γ-Al_2O_3 [31,33] were recorded under $^{12}CO/H_2O$ steady-state reaction conditions (Fig. 3a). The important characteristics of these spectra is the fact that *more than two* IR bands were recorded under $^{12}CO/H_2O$ reaction conditions, whereas two IR bands gave the red isotopic shift (2996 to 2989 cm^{-1} and 2903 to 2892 cm^{-1}, see Fig. 3a) and one IR band (2940 cm^{-1}) did not. It is noted that for a given type of COOH species (given coordination, see Section 3.2.3), two vibrational modes are expected in this range, νCH and δCH + νOCO_a [31]. It was not important in this work to perform accurate deconvolution and curve fitting procedures to resolve the number of different kinds of formate species that gave rise to the IR spectra seen in Fig. 3a. The clear understanding from the results of Fig. 3a is that there is at least one likely active formate species that gives the red ^{13}C-isotopic shift and another one that must be considered as inactive intermediate and which does not give the red isotopic shift.

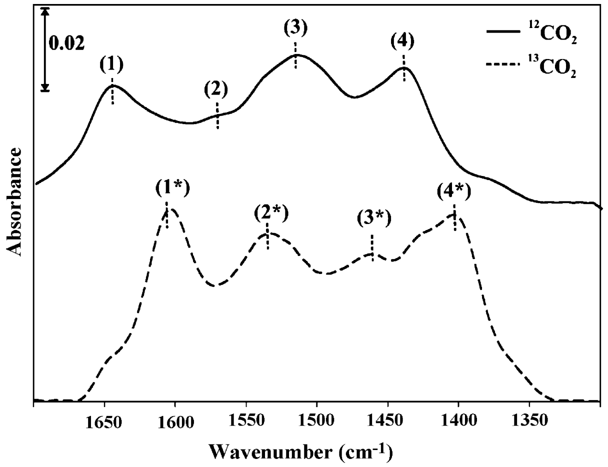

Fig. 4. DRIFTS spectra recorded in the 1700–1300 cm^{-1} range after treatment of the 0.5 wt.% Pt/γ-Al_2O_3 catalyst with 0.5%$^{12}CO_2$/Ar mixture (solid spectrum) and 0.5%$^{13}CO_2$/Ar mixture (dashed spectrum) for 20 min at 350 °C.

The most intense IR bands were recorded at 1594 (band 1) and 1391 (band 5) cm^{-1} under the $^{12}CO/H_2O$ reaction mixture (Fig. 3b, top graph), after deconvolution of the spectrum was made, and which could potentially be assigned either to OCO_{as} and OCO_s vibrational modes of formate species or to carbonates [16,17,30–33] depending on the chemical composition of support used and more importantly on the details of its surface microstructure on the atomic scale. Since the intensity of these bands is about 10 times stronger than those reported in Fig. 3a (νCH, exclusively to formate), and the ^{13}C red isotopic shift corresponding to the OCO vibrational modes is larger than that of νCH (see Fig. 3a and b, bottom graph), it would be more accurate to analyze the transient behavior of formate species based on the latter vibrational mode if we know that on the present catalyst and experimental conditions used it is possible to differentiate between the two adsorbed species (formate versus carbonates). For this reason we have designed and performed *in situ* $^{12}CO_2$ and $^{13}CO_2$ chemisorption DRIFTS experiments to be described in Section 3.2.2.

After the new steady-state (under the isotopic gas mixture $^{13}CO/H_2O$) was reached (Fig. 3b, bottom graph), it is clearly seen that in the region 1650–1500 cm^{-1} there exists *one IR band* that gave the red isotopic shift (band 1′) and a second one that did not show this isotopic shift (band 1). In the following Section 3.2.2, we will discuss the origin of these two IR bands. The infrared band at 1529 (band 2, Fig. 3b) corresponds to $O{-}C{-}O_{as}$ of carboxylate species [16,17,30–32], which is considered as *inactive* adsorbed species (no isotopic shift is observed). The infrared bands at 1485 (band 3, Fig. 3b) and 1439 (band 4, Fig. 3b) cm^{-1} correspond to unidentate carbonates [16,17,30–32]. It is seen that both kinds of carbonates do not give the isotopic shift. Therefore, these carbonate species are also considered as *inactive (spectator)* intermediates of the reaction. This is an important mechanistic result that points out that gaseous CO_2 produced under steady-state WGSR at 350 °C interacts *irreversibly* with O_L (support surface lattice oxygen) to form carbonates on the alumina surface.

3.2.2. *In situ $^{12}CO_2$ and $^{13}CO_2$ chemisorption DRIFTS studies*

After calcination (20%O_2/He, 600 °C, 2 h) of the Pt/γ-Al_2O_3 catalyst in the DRIFTS cell (~40 mg) followed by purge in Ar flow, the catalyst sample was cooled to 350 °C under Ar and the feed was then switched to a 0.5 vol.% $^{12}CO_2$/Ar gas mixture. The latter value of carbon dioxide composition used was larger than the steady-state concentration of CO_2 measured (0.32 vol.%) at the outlet of DRIFTS cell during WGSR conditions (see Section 3.2.1). Fig. 4

(upper graph) reports the infrared spectrum recorded. Following exactly the same CO_2 chemisorption procedure with another sample (~40 mg) of Pt/Al_2O_3 but using 0.5 vol.% $^{13}CO_2/Ar$ gas mixture the spectrum reported in Fig. 4 (bottom graph) was recorded. These CO_2 chemisorption-DRIFTS experiments provided the following important results and conclusions:

(a) The red ^{13}C-isotopic shifts due to the various kinds of carbonate species that could be formed on the alumina support upon CO_2 chemisorption are now available based on experimental evidence and not on literature reported values.
(b) The strong IR band 5′ recorded at 1360 cm^{-1} under the WGS reaction with ^{13}CO (Fig. 3b, bottom graph) *is not obtained* under the $^{13}CO_2/Ar$ chemisorption (Fig. 4, bottom graph) experiment.
(c) The maximum intensities of the IR bands corresponding to various kinds of chemisorbed CO_2 species observed in Fig. 4 appear about five times lower than those observed under the WGS reaction conditions (Fig. 3b) if no formate species produced is assumed. Considering the larger $CO_2(g)$ concentration used in the CO_2 chemisorption-DRIFTS experiments than that present under the WGS reaction, it is logical to assume that the surface concentration of chemisorbed CO_2 in the case of Fig. 4 is at least five times lower than that corresponding to Fig. 3b (assuming that no formate species were present).
(d) Based on point (b) mentioned above, it is safe to conclude that the strong IR band appeared at 1360 cm^{-1} under the $^{13}CO/H_2O$ reaction is due to a *formate species* ($O^{13}CO$ vibrational mode) *and not to carbonate* for the present catalytic system. Therefore, the strong IR bands 1 and 1′ appeared in Fig. 3b are *mostly due to formate* and to a lesser extent to carbonate species.

The IR bands 1 and 4 (1645 and 1440 cm^{-1}) recorded under the $^{12}CO_2/Ar$ gas mixture and shifted to 1603 and 1404 cm^{-1}, respectively, under the $^{13}CO_2/Ar$ gas mixture, correspond to a bicarbonate-type chemisorbed carbon dioxide, whereas the IR bands 2 and 3 recorded at 1570 and 1515 and shifted to 1530 and 1462, respectively, correspond to monodentate-type chemisorbed CO_2 (Fig. 4) [34].

3.2.3. SSITKA-mass spectrometry-DRIFTS (operando) WGS reaction

Fig. 5 shows transient response curves in terms of normalized concentration (*Z*) of $^{12}CO(g)$ and $^{12}CO_2(g)$ "carbon-containing" species recorded under the isotopic switch $3\%^{12}CO/10\%H_2O/Ar/He$ (350 °C, 30 min) → $3\%^{13}CO/10\%H_2O/Ar$ (350 °C, t) with mass spectrometry (*operando* studies). The Z-$^{12}CO_L(s)$ and Z-$^{12}COOH(s)$ response curves shown in Fig. 5 were estimated from the DRIFTS spectra recorded every 12 s (use of MCT detector) based on the 2033 and 1594 cm^{-1} ($O–^{12}C–O$) maximum band intensity, respectively, under the $^{13}CO/H_2O/Ar$ reaction mixture (Figs. 2a and 3b, respectively) according to the following relationship:

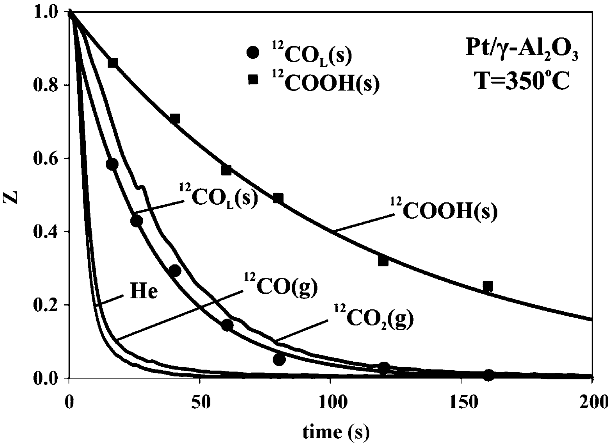

Fig. 5. Normalized concentration (*Z*) versus time transient response curves of ^{12}C-labelled gaseous CO and CO_2, and adsorbed CO_L and –COOH species found in the "C-path" of the WGS reaction on the 0.5 wt.% Pt/γ-Al_2O_3 catalyst at 350 °C. All responses were recorded during *operando* SSITKA studies.

$$Z = \frac{(I_{abs}(t) - I_{abs}(\infty))}{(I_{abs}(0) - I_{abs}(\infty))} \qquad (2)$$

where $I_{abs}(0)$ and $I_{abs}(\infty)$ refer to the absorbance recorded for $^{12}CO_L$ and $^{12}COOH(s)$ at steady-state under the $^{12}CO/H_2O$ and $^{13}CO/H_2O$ gas mixture, respectively. All gaseous and adsorbed surface responses were recorded simultaneously by *on line* mass spectrometer-DRIFTS (*operando*). It is important to state here that in the case of the IR band at 1594 cm^{-1} which arises from both formate and carbonate species (Fig. 4), the use of Eq. (2) to quantify the formate species is valid. This is true because the *Z* function considers the *net absorbance* signal after subtracting $I_{abs}(\infty)$, which is the residual absorbance *at any given time* under the $^{13}CO/H_2O$ gas mixture, due to the carbonates and formates that *do not participate at all* in the reaction path of the WGS reaction. In other words, the decrease of the $I_{abs}(t)$ at 1594 cm^{-1} with time in the $^{13}CO/H_2O$ gas mixture is due only to formate species that have been interacted with ^{13}CO as will be further discussed below.

In Fig. 5 it is clearly seen that the CO(g) response lags behind that of He, which is partly associated with the fact that some concentration of adsorbed ^{12}CO on the catalyst surface under steady-state WGSR conditions exchanges with gaseous ^{13}CO, while $^{12}CO(g)$ still continues to react during the first 45 s of the transient ($Z_{He} = 0$ at $t \sim 45$ s) to give $^{12}CO_2(g)$. The former explanation is in harmony with the SSITKA-DRIFTS results presented in Fig. 3 and previously discussed. Also, the $CO_L(s)$ response curve lags behind that of CO(g) (Fig. 5) since except that simple exchange of $CO_L(s)$ with gaseous CO takes place (Fig. 2), the former must also be considered as a *precursor intermediate* that forms –COOH, the latter decomposing/reacting to form $CO_2(g)$ and $H_2(g)$.

In Fig. 5 it is shown that the $^{12}COOH(s)$ transient response curve lags behind that of $^{12}CO_2(g)$. If $CO_2(g)$ is assumed to be formed via formate decomposition, then the opposite behavior would have been expected (e.g., the $^{12}CO_2(g)$ response curve to lag behind that of $^{12}COOH(s)$). The relative position of $^{12}COOH(s)$ transient response curve compared to that of $^{12}CO_2(g)$ (Fig. 5) can be explained based on the following mechanistic scheme:

$$CO(g) + s \leftrightarrow CO(s) \qquad (3)$$

$$CO(s) + OH(s)^{I} \leftrightarrow COOH(s)^{I} + s \qquad (4)$$

$$CO(s) + OH(s)^{II} \rightarrow COOH(s)^{II} + s \qquad (5)$$

$$COOH(s)^{II} \rightarrow CO_2(g) + H(s) \qquad (6)$$

$$2H(s) \rightarrow H_2(g) + 2s \qquad (7)$$

Reaction steps (4) and (5) indicate that adsorbed CO on the catalyst surface interacts with *two different* hydroxyl groups on the alumina support surface, according to the results of Fig. 1a and the discussion previously offered [21]. The CO(s) interaction with hydroxyl group, $OH(s)^{I}$ (step (4)) is considered *reversible*, whereas CO(s) can also interact *irreversibly* by another kind of hydroxyls, $OH(s)^{II}$ (step (5)). The latter interaction leads in turn to an irreversible decomposition of formate to form $CO_2(g)$ and $H_2(g)$

(steps (6) and (7)). Elementary step (6) was proposed to be the rate-determining step over the Pt/CeO_2 catalyst based on D-isotopic kinetic studies [32].

On the other hand, the first kind of formate species, $COOH(s)^{I}$ (step (4)) cannot be decomposed. If formate decomposition (step (6)) requires the presence of noble metal, then the latter $COOH(s)^{II}$ species must reside in a region away from the periphery of Pt-alumina interface. When the $^{13}CO/H_2O$ mixture is switched over the catalyst, $^{12}COOH(s)^{I}$ species formed under the $^{12}CO/H_2O$ treatment is expected to be replaced by $^{13}COOH(s)^{I}$ according to reaction steps (3) and (4). This process will contribute to the reduction of the IR band recorded at 1594 cm^{-1}. On the other hand, the active $^{12}COOH(s)^{II}$ species will be replaced by the equivalent $^{13}COOH(s)^{II}$ (step (5)), which in turn will produce $^{13}CO_2(g)$ (step (6)), and this process will also contribute to the diminishing of IR band at 1594 cm^{-1} (Fig. 3b). Each of the two processes described above involving $COOH(s)^{I}$ and $COOH(s)^{II}$ should be governed by different kinetics.

Based on the above reaction scheme (steps (3–7)) and the discussion offered, the $^{12}COOH(s)$ transient response curve of Fig. 5 can be seen as the result of the sum of two transient rates of $^{12}COOH(s)$ disappearance due to *two kinds of formate species* that gave the observed red isotopic shift (Fig. 2c). Only the second species $COOH(s)^{II}$ that leads to the formation of $CO_2(g)$ and $H_2(g)$ is considered to be a *true active* reaction intermediate, while the first one, $COOH(s)^{I}$, is simply a *spectator* species. The latter can exchange with $^{13}CO(g)$ via reaction steps (3) and (4). Therefore, the transient response curve of $^{12}COOH(s)^{II}$ would normally be expected to lie before the observed $^{12}CO_2(g)$ response considering that the latter is formed via formate decomposition. The performance of kinetic analysis and deconvolution of the observed $^{12}COOH(s)$ transient response curve that would allow to produce the two transient response curves of $^{12}COOH(s)^{I}$ and $^{12}COOH(s)^{II}$ previously discussed was out of the scope of the present work.

Meunier et al. [20,35] have recently reported on the same behavior of $^{12}CO_2(g)$ and $^{12}COOH(s)$ SSITKA response curves shown in Fig. 5, in that the $^{12}CO_2(g)$ transient response curve lagged behind that of $^{12}COOH(s)$ over a 2 wt.% Pt/CeO_2 catalyst at 160 °C. At a higher temperature (T = 220 °C) the above behavior was not seen. The authors have proposed that formate species was an *inactive* reaction intermediate at 160 °C but an *active* one at 220 °C. However, the authors did not provide any explanation as what is the kinetic reason for the observed *slow decay* of $^{12}COOH(s)$ with time under the $^{13}CO/H_2O$ isotopic switch.

The proposed reaction scheme (steps (3–7)) and the discussion previously offered provide for *the first time* a very reasonable kinetic and mechanistic explanation of the slow decay of transient depletion of the concentration of ^{12}C-containing formate species measured by FTIR during a SSITKA-WGS reaction experiment. It is also mentioned here that Jacobs and Davis [36] also provided evidence for the participation of two kinds of –OH species according to their SSITKA-DRIFTS studies of the reverse WGS reaction on Pt/CeO_2 that involved formate as a *true active* reaction intermediate species.

In a recent DRIFTS-SSITKA study on Pt- and Au-based catalysts for the WGSR, Meunier et al. [37] have attempted to quantify the specific rate of formate decomposition based on the DRIFTS data and the specific rate of CO_2 formation measured by GC analysis of the outlet of the DRIFTS cell (*operando*). The purpose of this methodology which is logical was to better ascribe the role of formates whether should be considered as active or inactive reaction intermediates. However, based on the present analysis (reaction steps (3–7)) and the discussion offered for the slow decay of the observed formate transient response curve (Fig. 5), similar to that observed [37], it is questionable the correctness of their analysis since not all the measured concentration of formates may represent *true active* formate species. It is rather clear that a more advanced mechanistic and kinetic analysis of the SSITKA-DRIFTS experiment is required for such a case coupled with more experimental evidence as obtained in the present work (Figs. 3–5).

Based on the results of Fig. 2a and b, all kinds of adsorbed CO gave the red isotopic shift. However, based only on this result one cannot ascribe that all these species could be considered as active reaction intermediates. The reversible nature of CO chemisorption on supported-Pt catalysts strongly implies that the red isotopic shift could also be due to a simple exchange reaction:

$$^{12}CO(s) + {}^{13}CO(g) \leftrightarrow {}^{13}CO(s) + {}^{12}CO(g) \qquad (8)$$

It is therefore impossible based only on the SSITKA-DRIFTS experiment (Fig. 2) to identify which of the CO(s) species are *true active* reaction intermediates. On the other hand, *at least one* CO(s) must be considered as an *active* intermediate that participates in the mechanism of WGSR.

3.3. Probing the back-spillover of OH/H species

Fig. 6 presents transient response curves of $H_2(g)$, $D_2(g)$ and HD(g) obtained at 500 °C under the 3%CO/10%H_2O/Ar (500 °C, t) treatment of the catalyst according to the sequence described in Section 2.4. Integration of the transient response curves of $D_2(g)$ and HD(g) provides the amount of D species (μmol/g). This was found to be 138 μmol D/g or equivalent to 11.2 monolayers of surface Pt ($\theta_D = 11.2$). It is therefore very clear that the large amount of D species measured, in harmony with the SSITKA results of Fig. 1a and those previously reported at 500 °C [21], cannot reside on Pt. It is strongly suggested that OD/D species are able to diffuse on the alumina surface at 500 °C and participate in the water-gas shift reaction by the aid of Pt (back-spillover of OH/H species). As discussed in the previous section, participation of OH is necessary for the formation of formate species (step (5)). The latter is energetically able to decompose to $CO_2(g)$ and H(s) by the aid of Pt (step (6)) [21]. It is important to note that under the 10-min treatment of the catalyst in Ar flow at 500 °C no $D_2(g)$ or HD(g) was observed, strongly suggesting that at 500 °C the interaction of –OH groups present on the alumina and the Pt surface (if any) does not lead to the production of any $H_2(g)$.

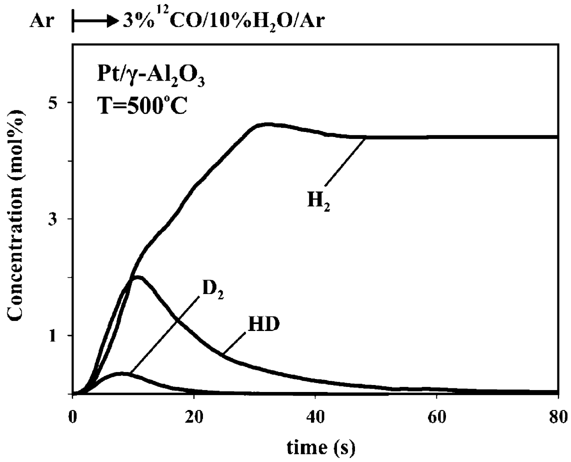

Fig. 6. Transient isotopic experiment that probes the back-spillover of OH/H species from the alumina to the Pt surface under WGS reaction on the 0.5 wt.% Pt/γ-Al_2O_3 catalyst. Sequence of steps: 10%D_2O/Ar (500 °C, 30 min) → Ar (500 °C, 10 min) → 3%^{12}CO/10%H_2O/Ar (500 °C, t). The transient response curves of $H_2(g)$, $D_2(g)$ and HD(g) produced under the last step are shown.

4. Conclusions

The following main conclusions can be derived from the results of the present work:

- The mechanism of the WGSR on the 0.5 wt.% Pt/γ-Al_2O_3 catalyst (D_{Pt} = 48%) passes through the formation of one active and one inactive intermediate formate species. The latter is formed in a reversible manner from the interaction of surface CO and –OH groups of the alumina support. Both species give the red isotopic shift upon the SSITKA switch $^{12}CO/H_2O \rightarrow {}^{13}CO/H_2O$ at 350 °C. Inactive formate species are also formed in an irreversible manner by the interaction of surface CO and different kinds of –OH groups present on the alumina support surface.
- *Operando* SSITKA-DRIFTS-mass spectroscopy studies of the WGS reaction on the 0.5 wt.% Pt/γ-Al_2O_3 catalyst revealed the presence of a large concentration (μmol/g) of *active* OH/H species on the alumina support, and a much smaller concentration of *active* adsorbed CO on Pt and formate species on the alumina close to the Pt-alumina interface.
- The accumulation of a large concentration of OH/H species on the alumina surface under steady-state WGS reaction conditions may imply a small rate constant associated with the diffusion of these species towards catalytic sites in the "H-path" of the reaction mechanism [21].
- The back-spillover of OH/H species from the alumina to the Pt surface under WGS reaction conditions was evidenced by partially labeling the alumina surface with –OD groups followed by reaction in CO/H_2O. A large amount of HD(g) and D_2(g) was measured (θ_D = 11.2).

Acknowledgements

The financial support of the European Committee (6th FP, no. 5183309 (SES6)) and the Research Committee of the University of Cyprus is gratefully acknowledged.

References

[1] R. Farrauto, S. Hwang, L. Shore, W. Ruettinger, J. Lampert, T. Giroux, Y. Liu, O. Ilinich, Annu. Rev. Mater. Res. 33 (2003) 1.
[2] A.B. Mhadeshwar, D.G. Vlachos, Catal. Today 105 (2005) 162.
[3] C. Rhodes, B. Peter Williams, F. King, G.J. Hutchings, Catal. Commun. 3 (2002) 381.
[4] Q. Fu, H. Saltsburg, M. Flytzani-Stephanopoulos, Science 301 (2003) 935, and references therein.
[5] D. Duprez, Catal. Today 112 (2006) 17, and references therein.
[6] G. Jacobs, A.C. Crawford, B.H. Davis, Catal. Lett. 100 (2005) 147, and references therein.
[7] T. Bunluesin, R.J. Gorte, G.W. Graham, Appl. Catal. B: Environ. 15 (1998) 107.
[8] R.J. Gorte, S. Zhao, Catal. Today 104 (2005) 18.
[9] S. Hilaire, X. Wang, T. Luo, R.J. Gorte, J. Wagner, Appl. Catal. A: Gen. 215 (2001) 271.
[10] Y. Li, Q. Fu, M. Flytzani-Stephanopoulos, Appl. Catal. B: Environ. 27 (2000) 179.
[11] W. Liu, M. Flytzani-Stephanopoulos, J. Catal. 153 (1995) 317.
[12] B. Aeijelts Averink Silberova, G. Mul, M. Makkee, J.A. Moulijn, J. Catal. 243 (2006) 171.
[13] E. Chenu, G. Jacobs, A.C. Crawford, R.A. Keogh, P.M. Patterson, D.E. Sparks, B.H. Davis, Appl. Catal. B: Environ. 59 (2005) 45.
[14] G. Jacobs, U.M. Graham, E. Chenu, P.M. Patterson, A. Dozier, B.H. Davis, J. Catal. 229 (2005) 499.
[15] G. Jacobs, L. Williams, U. Graham, D. Sparks, B.H. Davis, J. Phys. Chem. B 107 (2003) 10398.
[16] G. Jacobs, L. Williams, U. Graham, G.A. Thomas, D.E. Sparks, B.H. Davis, Appl. Catal. A: Gen. 252 (2003) 107.
[17] T. Shido, Y. Iwasawa, J. Catal. 141 (1993) 71, and references therein.
[18] D.C. Grenoble, M.M. Estadt, D.F. Ollis, J. Catal. 67 (1981) 90.
[19] S. Ricote, G. Jacobs, M. Milling, Y. Ji, P.M. Patterson, B.H. Davis, Appl. Catal. A: Gen. 303 (2006) 35.
[20] F.C. Meunier, D. Tibiletti, A. Goguet, S. Shekhtman, C. Hardacre, R. Burch, Catal. Today 126 (2007) 143, and references therein.
[21] G.G. Olympiou, C.M. Kalamaras, C.D. Zeinalipour-Yazdi, A.M. Efstathiou, Catal. Today 127 (2007) 304, and references therein.
[22] K. Polychronopoulou, C.N. Costa, A.M. Efstathiou, Appl. Catal. A: Gen. 272 (2004) 37.
[23] C.M. Kalamaras, A.M. Efstathiou, J. Catal., to be submitted for publication.
[24] A.M. Efstathiou, X.E. Verykios, Appl. Catal. A: Gen. 151 (1997) 109.
[25] B.C. Smith, Fundamentals of fourier transform infrared spectroscopy, CRC Press, 1996.
[26] J. Sirita, S. Phanichphant, F.C. Meunier, Anal. Chem. 79 (2007) 3912.
[27] D. Tessier, A. Rakai, F. Bonzon-Verduraz, J. Chem. Soc., Faraday Trans. 88 (1992) 741.
[28] K. Almusaiter, S.S.C. Chuang, J. Catal. 180 (1998) 161.
[29] A.M. Bradshaw, H. Hoffman, Surf. Sci. 72 (1978) 513.
[30] G. Jacobs, A. Crawford, L. Williams, P.M. Patterson, B.H. Davis, Appl. Catal. A: Gen. 267 (2004) 27.
[31] G. Busca, J. Lamotte, J.-C. Lavalley, V. Lorenzelli, J. Am. Chem. Soc. 109 (1987) 5197, and references therein.
[32] G. Jacobs, S. Khalid, P.M. Patterson, L. Williams, D. Sparks, B.H. Davis, Appl. Catal. A:Gen. 268 (2004) 255.
[33] O. Demoulin, M. Navez, P. Ruiz, Appl. Catal. A: Gen. 295 (2005) 59, and references therein.
[34] G. Busca, V. Lorenzelli, Mater. Chem. 7 (1982) 89.
[35] F.C. Meunier, D. Tibiletti, A. Goguet, R. Burch, Oil Gas Sci. Technol. 61 (2006) 497.
[36] G. Jacobs, B.H. Davis, Appl. Catal. A: Gen. 284 (2005) 31.
[37] F.C. Meunier, A. Goguet, C. Hardacre, R. Burch, D. Thompsett, J. Catal. 252 (2007) 18.